Anomalous Diffusion of Sand Tracer Particles Under Waves

Gregory W. Wilson

[1]Oregon State University, College of Earth Ocean and Atmospheric Sciences, 104 CEOAS Administration Building, Corvallis, OR , 97331-5503

Key Points:

- Stochastic theory is developed for dispersal of sand in wave-driven vortex ripples
- Theory predicts anomalous (non-classical) dispersion of the sediment tracer plume
- Theory is verified using re-analysis of previous flume and ocean sediment tracer experiments

Corresponding author: 1, `wilsongr@coas.oregonstate.edu`

Abstract

A model is presented for the horizontal and vertical diffusion of sand tracer particles by waves, and is verified using a re-analysis of the experiments of *Miller and Komar* [1979]. In the model, sand particles take random jumps at a rate associated with the wave period, but also can bury one another resulting in intermittent long rest times between jumps. The particle jump length between burials is modeled by considering a vortex entrainment and advection mechanism, resulting in a probability distribution as a function of wave orbital excursion amplitude and particle settling velocity. The model is formalized using the theory of continuous time random walks to obtain closed-form expressions for the horizontal particle spreading rate, and plume shape, without tunable parameters. Importantly, the model predicts sub-diffusive particle spreading, a previously unconsidered phenomenon that is apparent in the experimental data. The plume horizontal extent versus time is also well-predicted compared to experimental data.

1 Introduction

The Lagrangian approach to sediment transport aims to describe the trajectories of sediment particles driven by a fluid flow, as would be measured by tracking tagged sediment or "tracers". Such measurements were widely used in early studies of nearshore wave-driven sediment transport [*Inman and Chamberlain*, 1959; *Komar and Inman*, 1970; *Ingle and Gorsline*, 1973]. Although tracer use has declined in nearshore research following the development of high-resolution Eulerian sediment flux sensors [*White*, 1998], which measure time-dependent sediment concentration and flux at a fixed station, they are still preferred for problems that consider a broad range of spatial/temporal scales. For instance, tracers are favored for monitoring the long-term and large-scale dispersal of dredge placements [*McComb and Black*, 2005], where Eulerian measurements or model simulations are impractical. They are a natural fit for monitoring the redistribution of sediments from a localized source (whether natural or anthropogenic), or the fate of certain contaminants which exist preferentially in a sediment-bound phase (e.g., radioisotopes, heavy metals). And tracers can be used to monitor transport of cobble- and gravel-sized sediment for which few other observational techniques exist [*Osborne*, 2005; *Allan et al.*, 2006; *Stark and Hay*, 2016].

The interpretation of tracer measurements requires a Lagrangian theory that predicts time-dependent statistics (e.g., spatial mean and standard deviation) of an ensemble of tracer particles travelling over the seabed, accounting for both advection and diffusion processes. However, no general theory for sediment diffusion currently exists. The classical advection-diffusion equation is often invoked when analyzing tracer data, but here the diffusive process is generally treated empirically, i.e. by fitting the particle diffusivity to data. Predicting diffusion from first principles requires considering sediment entrainment, stirring (e.g., by turbulent eddies and Taylor dispersion), and deposition and burial. *Mei and Chian* [1994] derived analytical equations for turbulent sediment diffusion in an oscillatory boundary layer, valid for very small particles that do not undergo deposition or burial. *Mazumder and Paul* [2012] developed a similar numerical model that included particle deposition, which they found caused a significant reduction in diffusion. *Soulsby et al.* [2007] adopted a more practical approach, by directly simulating particle trajectories within a full-scale coastal model, and using stochastic representations for burial, entrainment, and stirring. This latter approach highlighted the role of stochastic parameterization in predictive models for Lagrangian sediment transport, due to the fact that coastal models do not resolve the boundary layer processes responsible for diffusion. The stochastic approach has also been studied on a more fundamental level by *Komar* [1969], who modeled wave-driven stirring as a classical random walk process, and *Pizzuto* [1987], who directly simulated a similar random walk model, including particles with different diffusion coefficients which they attributed to different modes of transport (suspended and bed-load).

Stochastic models for Lagrangian sediment transport, such as the ones just described, all have their basis in a random walk description [*Einstein*, 1937] where each sediment particle is assumed to execute a series of jumps of random length separated by random rest time periods. An application of the central limit theorem then shows that the distribution of an ensemble of such particles is governed by the classical advection diffusion equation. Recent developments in Lagrangian sediment transport theory have challenged this by invoking the possibility of jump length and/or rest time probability distributions that include large intermittent events. In particular, heavy-tailed distributions (whose tails decay as $x^{-\alpha-1}$ with $0 < \alpha < 2$) lack a finite second moment, and the central limit theorem no longer applies. *Metzler and Klafter* [2000] described the more-general theory governing diffusion in this case, and *Schumer et al.* [2009] reviewed the main results as they apply to sediment transport. The theory shows that heavy-tailed jump length distributions result in heavy-tailed particle excursion distributions, and heavy-tailed rest time distributions result in anomalously slow spreading (standard deviation increases slower than $t^{1/2}$). Some possible physical causes for heavy-tailed jump length distributions include the influence of heterogeneous flow or topography at the scale of particle motion [*Tucker and Bradley*, 2010], or differing mobility within mixed-size sediments [*Ganti et al.*, 2010; *Hill et al.*, 2010]. Heavy-tailed rest time distributions may be caused by particles being intermittently trapped or buried [*Parker et al.*, 2000; *Voepel et al.*, 2013; *Martin et al.*, 2014; *Pelosi et al.*, 2014, 2016]. Both types of anomalous diffusion behavior have been observed for sediment transport in streams [*Nikora et al.*, 2002; *Bradley et al.*, 2010], and the microscopic (particle-scale) statistics which underlie the anomalous macroscopic behavior have also been the subject of experiments [*Drake et al.*, 1988; *Habersack*, 2001; *Ancey et al.*, 2006; *Lajeunesse et al.*, 2010; *Martin et al.*, 2012; *Roseberry et al.*, 2012; *Hassan et al.*, 2013; *Heyman et al.*, 2013; *Radice et al.*, 2013; *Ballio and Radice*, 2015; *Fathel et al.*, 2015; *Wilson and Hay*, 2016] and theories [*Ancey et al.*, 2008; *Ancey*, 2010; *Furbish and Schmeeckle*, 2013; *Fan et al.*, 2014, 2016]. It should be noted that the root causes of anomalous diffusion have, in large part, eluded direct verification, e.g. via observations of heavy-tailed jump length distributions, and this remains an ongoing area of research.

It is unknown whether anomalous sediment diffusion occurs for wave-driven transport, as it does in streams. If so, this would affect the interpretation of sediment tracer observations, as well as model predictions that assume classical advection-diffusion behavior. With that in mind, the goal of the present work is to develop a basic statistical model for particle diffusion starting from a random walk description, where the diffusion is assumed to be due to sediment exchange amongst vortex ripples (the latter assumption being motivated in part by the available experimental data). The model includes an explicit representation of particle burial, which results in a heavy-tailed rest time distribution. This is illustrated in a simple conceptual framework showing that burial causes sub-diffusion with a plume width (as measured by standard deviation) growing as $t^{1/4}$. The conceptual model is then generalized as a continuous time random walk (CTRW), with a jump length probability distribution based on existing sediment transport parameterizations over vortex ripples. In section 4, the CTRW model is used to re-analyze sediment tracer data collected by *Miller and Komar* [1979] (section 3), whose experiments considered pure sediment diffusion (i.e., no advection) by waves over self-generated vortex ripples. The data exhibit a clear signature of anomalous sub-diffusion, which would not be predicted by a classical advection-diffusion model, but is well-predicted by the proposed CTRW model. The space/time scales for diffusion, which derive from the proposed jump length probability distribution, are also found to agree well with observations.

2 Theory

The sediment diffusion theory will be developed in three sections. First, section 2.1 introduces the conceptual approach used, including the main assumptions and approximations, leading to a basic stochastic model for simulating sediment diffusion. Section 2.2 applies

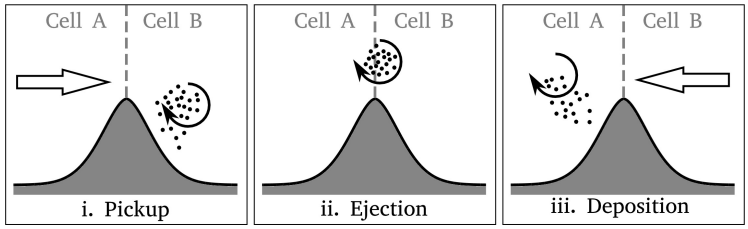

Figure 1. Sketch of conceptual model discretizing vortex ripples into cells that exchange coherent packets of sediment. Open arrows indicate free stream flow direction. The vortex entrainment and exchange mechanism is shown, comprising (i) pickup of a coherent packet of sediment by the lee vortex during the forward wave stroke, (ii) ejection of this packet into the main flow during flow reversal, and finally (iii) advection and deposition of the packet downstream during the backward wave stroke. Only one vortex is shown, for clarity.

abstractions to this conceptual model, with the aim of deriving a closed-form solution for the distribution of particle displacements using the theory of continuous time random walks (CTRW). Finally, closure of the CTRW model requires a probability distribution for particle jump lengths, which is derived in section 2.3 based on existing sediment transport parameterizations.

2.1 Conceptual Model

The model concept is based on random sediment transport and exchange, driven by periodic wave motion. The bed is assumed to be infinitely deep and homogeneous, made of uniform sized particles, and in equilibrium with the driving flow. The model discretizes the bed into a one-dimensional array of cells, in which the cell spacing is equal to a characteristic excursion distance for an entrained particle during one wave stroke. In particular, in the present description the bed will be assumed to be organized into vortex ripples (also known as orbital-scale ripples), assumed to be in equilibrium and non-migrating. Each model cell corresponds to one ripple face, i.e. 1/2 ripple wavelength, as illustrated in Figure 1. Note that, unlike other cellular automata-like models designed to simulate the time evolution of wave-formed ripples [*Pannell et al.*, 2002; *Gallagher*, 2011], the present model is not designed to resolve the bed topography itself and the associated flow-topography feedbacks. Rather, the intent of the model is to represent the stochastic mobilization and redistribution of sediment amongst pre-existing ripples.

Sediment transport in vortex ripples was first described by *Bagnold and Taylor* [1946] and is illustrated (in a simplified form) in Figure 1. During each wave stroke a coherent vortex forms on the lee side of each ripple, then is subsequently ejected up into the water column around the time of flow reversal. These vortices drive bed-load sediment transport up the ripple crests, thereby reinforcing the ripple shape. They also entrain suspended sediment and thereby account for most of the suspended transport: once ejected, the sediment-laden vortices are advected by the wave flow by distances of one or more ripple wavelengths, all the while continually releasing sand. The path of the advected vortices can be approximated as passive advection by the wave orbital velocity, as has been documented using particle imaging velocimetry [*Earnshaw and Greated*, 1998; *Admiraal et al.*, 2006]. Sediment transport by the vortices has been quantified by *Nakato et al.* [1977] and *van der Werf et al.* [2007], who measured vertical profiles of sediment concentration at various fixed points along the ripple profile. Their time series observations show multiple distinct peaks in sediment concentration associated with the passage of the advected vortices. *Nakato et al.* [1977] observed two such peaks per wave stroke, while *van der Werf et al.* [2007] observed three, which they interpreted as advection over a distance of one or two ripple wavelengths respectively.

A simple conceptual model is proposed here for the vortex mechanism of sediment exchange between ripples. Transfers of sediment between ripple cells will be represented in terms of unit packets of an arbitrary average size (number of particles), similar to the "grab and dump" model of *Nielsen* [1988]. This corresponds to the basic description of vortex ripple sediment exchange discussed above, where suspended sediment is transported in coherent vortices as in Figure 1. For each wave stroke, one such packet is assumed to be mobilized from the surface of each ripple cell, and is transferred onto the surface of the adjacent downstream ripple cell with fixed probability $p < 1$. Furthermore, whenever a sediment packet is transferred from one ripple cell to another the deposited particles cause an equal number of particles in the receiving ripple cell to become buried, and such buried particles remain inactive until some combination of subsequent transfers causes them to rise back to the surface. The intra-ripple spatial distribution of this process is taken to be uniform, as explained in the Appendix. Additionally, wave-to-wave variability in the number of particles entrained is assumed to be averaged out over the course of multiple wave strokes.

The average distribution of horizontal particle excursions versus time can be calculated for this model by simulating a large number of particle trajectories while taking into account the interactions between particles by burial. It would appear that this simulation requires accounting for interactions between all surface particles in every ripple cell, but here is it assumed that the particles in each sediment packet are randomly mixed such that the same average distribution of particle interactions (and therefore particle trajectories) would be obtained if each ripple cell supported just one surface particle. Therefore, the overall distribution of trajectories can be approximated by an ensemble of model realizations having one particle per ripple cell. This simplifies the book-keeping associated with particle burial and exhumation, as each cell effectively maintains a last-in-first-out vertical stack of particles.

Numerical simulations of the above conceptual model were implemented using a periodic lattice of 1000 single-particle ripple cells in one horizontal dimension, for 450 wave cycles, and for 500 independent trials. The simulations used an arbitrary value of $p = 0.25$. In each wave stroke the simulation randomly assigns either transfer or non-transfer to each cell, and then sequentially executes each transfer and its associated burial. Horizontal and vertical trajectories were recorded for all of the particles that started on the bed surface. Figure 2 shows an example model simulation result illustrating how particles are redistributed, mixed, and buried over time. Figure 3 shows example time series of particle horizontal displacements for the same simulation, illustrating the fact that particles are occasionally inactive for long periods of time due to burial.

Statistics of the particle trajectories are shown in Figures 4–5. It is apparent that the burial process has a significant effect on spreading: particles are sometimes stationary (buried) for long periods of time, resulting in a variance growth rate that tends asymptotically to $t^{0.5}$ (Figure 4). That is, burial causes sub-diffusion, meaning variance growth that is slower than the linear rate predicted by classical diffusion. The distribution of particle displacements (Figure 5) features a cusp at $x = 0$, and light tails which decay faster than x^{-3}, as is expected for a sub-diffusive random walk process [*Klafter and Sokolov*, 2011].

2.2 Random Walk Model

The conceptual sediment diffusion model will now be further abstracted as a random walk on a continuous horizontal coordinate x, with a discrete vertical coordinate m used to represent the particle burial/exhumation process, and a time index $n = t/\Delta t$. The constraint that particles can only jump a distance of one ripple 1/2-wavelength per unit time will also be relaxed.

The geometry and concept of the random walk model is sketched in Figure 6. Consider a single particle at $x = 0$ which is initially ($n = 0$) on the bed surface $m = 0$. At time $n = 1$, exactly one of two events is assumed to occur: A"jump", in which the particle is transferred from $x = 0$ to $x = x'$, for some value of x'; or a "burial", in which a different particle

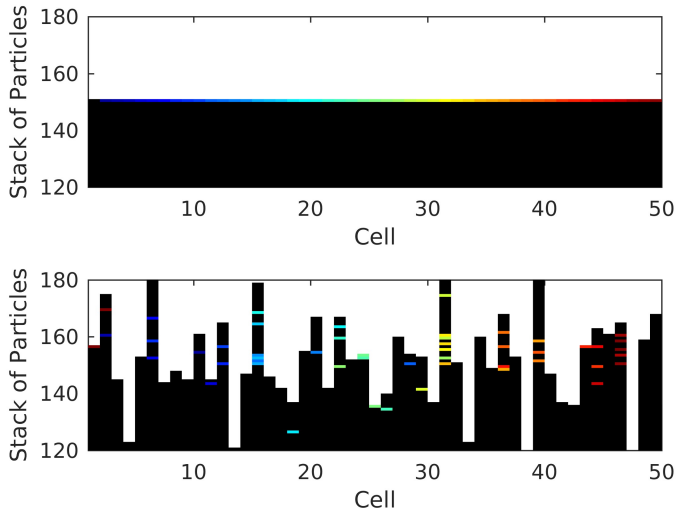

Figure 2. Example simulation using conceptual ripple cell model (section 2.1). Top: initial state, with surface particles marked by colors and non-surface particles in black (only the topmost part of the infinitely-deep bed is shown). Bottom: state after 450 wave cycles. In each wave 1/2 cycle, each ripple cell (horizontal gridpoint) transfers its surface particle to the adjacent downstream cell with finite probability. The particle burial/exhumation associated with these transfers results in a random horizontal and vertical redistribution of the marked particles. Note that the vertical scale is greatly exaggerated, being on the order of grain diameters, compared to the horizontal scale which represents ripple 1/2-wavelengths.

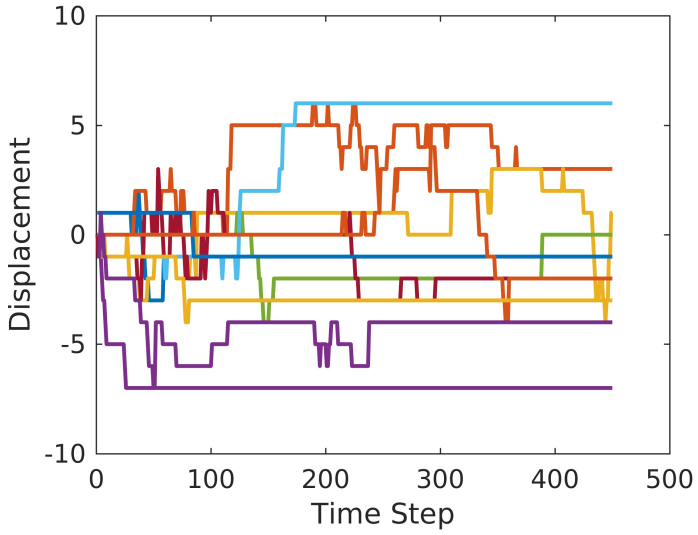

Figure 3. Example timeseries of horizontal particle displacements (measured in number of cells) for a simulation of the conceptual ripple cell model, as shown in Figure 2.

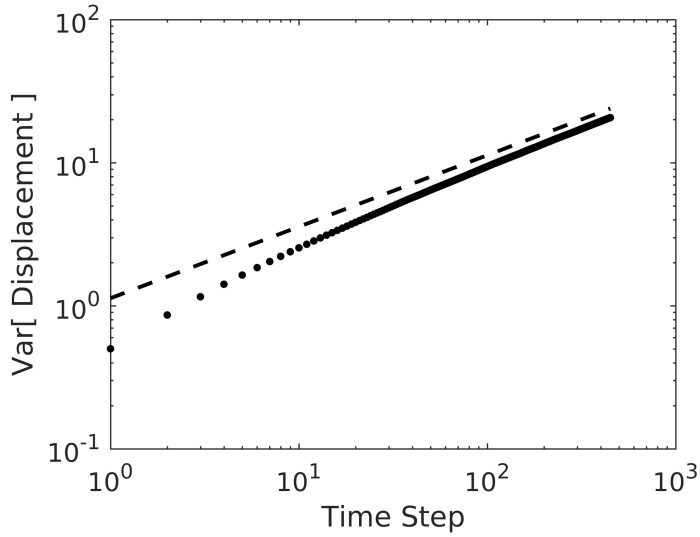

Figure 4. Variance of horizontal displacements (measured in number of cells) of initially surface particles in the conceptual ripple cell model, as a function of time. Solid line is $t^{0.5}$.

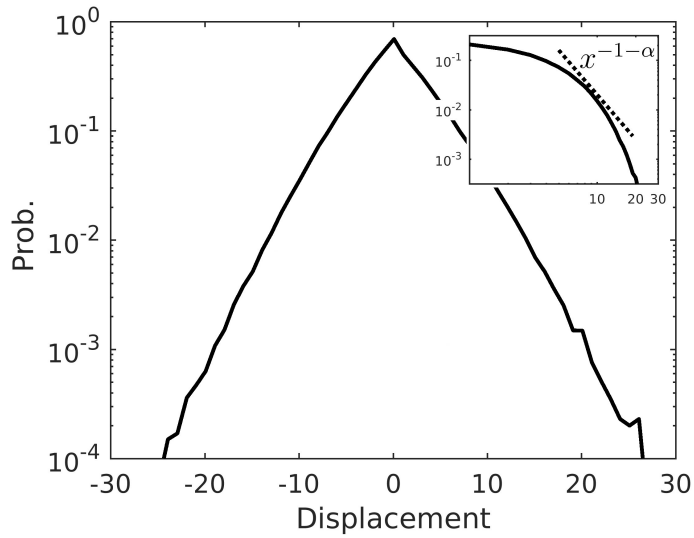

Figure 5. Estimated probability density function of horizontal displacements (measured in number of cells) of initially surface particles in the conceptual ripple cell model, after 450 wave cycles. Inset shows same data on log-log axis to illustrate tail behavior: dashed line shows heavy-tail limit $\alpha = 2$ for comparison.

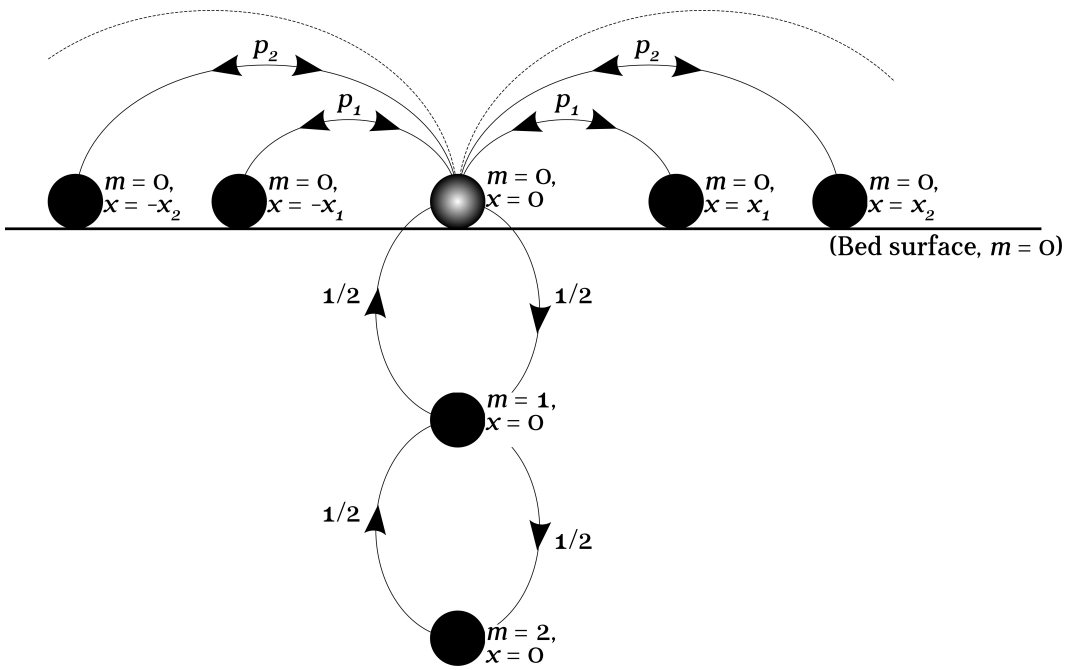

Figure 6. Coordinates and schematic for random walk particle model. At the next time step, the shaded particle at the bed surface will either jump horizontally ($x \rightarrow \pm x'$) or be buried vertically ($m \rightarrow m + 1$), with equal probability. Jumps can take on any distance x: several example jump trajectories are shown, labelled with their corresponding probabilities p_i. Burial can be caused by particles jumping to $x = 0$ from any distance x: the same example trajectories are shown to illustrate the symmetry in the jump/burial process. If buried, the particle then executes a random walk in m before being exhumed, which can also be modeled using the burial time probability distribution equation (1).

jumps from some location $x = x'$ to $x = 0$, causing the original particle to become buried (m increases from 0 to 1). By symmetry, "jump" and "burial" events are equally probable at time $n = 1$ for the particle at $x = 0$: the bed is assumed uniform and composed of identical particles, so the probability of a particle jumping from $x = 0$ to $x = x'$ is equal to that of a particle jumping from $x = x'$ to $x = 0$, for any x'. While the possibility of particles simultaneously entering and leaving the site $x = 0$ during one time step appears to have been neglected, this can be resolved by considering the model in terms of an ensemble of possible outcomes (jump or burial) for the single particle at $x = 0$, rather than as a lattice of mutually interacting particles as in the previous conceptual model.

Assuming the particle originally at $x = 0$ executes a jump at $n = 1$, it remains as a surface particle at its new position and thus repeats the same process at the next time step. If instead the original particle is buried at $n = 1$, the process repeats at $x = 0$ but for the new surface particle (i.e. the one which caused the burial), so that at the next time step the original particle may become further buried ($m = 2$), or may be exhumed ($m = 0$). Importantly, these two events also occur with equal probability due to the jump/burial symmetry noted previously. Continuing this process, it is apparent that a particle that jumps to a site x at time $n = 0$ subsequently executes a 1-dimensional random walk in the vertical direction [cf. *Voepel et al.*, 2013; *Martin et al.*, 2014], consisting of zero or more time steps with $m \geq 0$, followed by one jump event. The probability of $2n$ time steps occurring before the latter jump event is therefore equal to the first-return probability for a 1-d random walk [*Klafter and Sokolov*, 2011],

$$u_{2n} = \binom{2n}{n} \frac{2^{-2n}}{2n-1}. \tag{1}$$

In other words, u_{2n} describes the probability that a particle will rest for $2n$ time steps between successive jumps, i.e. it is the (discrete) rest time distribution. Stirling's approximation shows that for large n equation (1) tends to a power-law distribution $n^{-3/2}/2\sqrt{\pi}$. Therefore, an appropriate continuous probability density function for modeling the time between jump events is

$$p_T(t) = \frac{\alpha}{\Delta t} \left(\frac{t}{\Delta t}\right)^{-1-\alpha}, \tag{2}$$

where $\alpha = 1/2$ and $t \geq \Delta t$. Figure 7 shows that p_T has the same tail behavior as the discrete equation (1), and also approximates the probability mass for small n. Note that the parameter Δt represents the minimum time any particle stays at a given x position before either jumping or becoming buried, consistent with the previous description where a particle at the surface will experience either a jump or a burial within time Δt.

Similar to the rest time distribution p_T, a distribution p_X is assumed to exist for the particle jump lengths, although a specific model for p_X is deferred to section 2.3. The distributions p_X and p_T together specify a continuous-time random walk [CTRW; *Montroll and Weiss*, 1965], in which a particle's horizontal path consists of a series of random jumps separated by random rest times (in this case representing burial). The relevant theory has been reviewed by *Schumer et al.* [2009] with an eye towards sediment transport, as well as by *Metzler and Klafter* [2000] who provide some useful closed-form results. In particular, for a light-tailed jump length distribution p_X the spatial distribution of an ensemble of tracer particles originating from a point source tends asymptotically to

$$W(x,t) = \frac{1}{\sqrt{4K_\alpha t^\alpha}} \sum_{n=0}^{\infty} \frac{(-1)^n}{n!\Gamma\left(1-\alpha[n-1]/2\right)} \left(\frac{x^2}{K_\alpha t^\alpha}\right)^{n/2}, \tag{3}$$

where $\alpha = 1/2$ as in equation (2), and Γ is the Gamma function. The generalized diffusion constant K_α in equation 3 is defined as

$$K_\alpha = \frac{\sigma_x^2/2}{\Delta t^\alpha}, \tag{4}$$

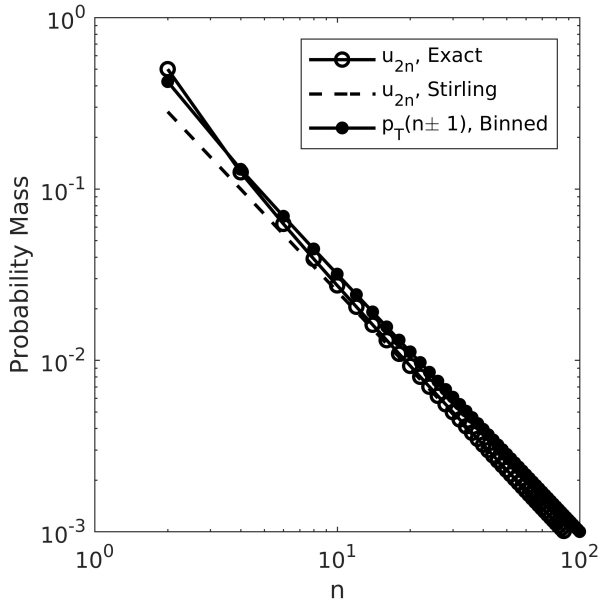

Figure 7. Comparison of equation (1), Stirling's approximation ($u_{2n} \approx n^{-3/2}/2\sqrt{\pi}$), and the continuous rest time distribution equation (2). The latter has been integrated over centered bins of width $2n$ to calculate a probability mass for comparison to u_{2n}.

where σ_x^2 is the jump length variance (based on p_X). Finally, the variance of horizontal particle excursions is given by

$$\sigma^2 = E[\Delta x^2] = \frac{2K_\alpha}{\Gamma(1+\alpha)} t^\alpha. \tag{5}$$

Note that the variance growth rate for classical diffusion is recovered when $\alpha = 1$, whereas the numerically simulated behavior of the conceptual model in section 2.1 (Figures 4–5) is recovered with $\alpha = 1/2$ as predicted by equation (2). This confirms that the abstraction of particle burial as a first-return random walk process (equation (2)) is indeed consistent with the more-intuitive conceptual model.

2.3 Particle Jump Length Distribution

Whereas p_T in the random walk model represents the particle burial and exhumation process, p_X describes the motions of particles in terms of their jump length distribution when they are mobilized. Recall that in the present case the particle "jumps" correspond to entrainment within a ripple lee vortex followed by subsequent advection by the wave orbital velocity and ending in deposition. *Nielsen* [1988] introduced a simple model for particle trajectories in this situation, based on the idea that particles are entrained into the flow instantaneously at the moment of flow reversal ($t = 0$), i.e. when the lee vortex is released into the flow. The time-averaged vertical distribution of these entrained particles can be approximated by

$$c(z) = c_0 e^{-z/L_0}, \tag{6}$$

which stems from particle setting being balanced by turbulent stirring with a constant eddy diffusivity. This model is supported by observations of the mean sediment concentration above both flat and rippled beds [e.g., *van der Werf et al.*, 2006]. The underlying assumption of constant sediment eddy diffusivity is generally valid in the lowermost part of the flow over rippled beds, where the transport is dominated by vortex shedding [*Thorne et al.*, 2009]. A

parameterization for the decay length L_0 was given by *Nielsen* [1992] as

$$L_0 = \begin{cases} 0.075\frac{U_0}{w_s}\eta, & \frac{U_0}{w_s} < 18 \\ 1.4\eta, & \frac{U_0}{w_s} > 18 \end{cases} \tag{7}$$

where U_0 is the free stream wave orbital velocity amplitude, w_s is the particle settling velocity, and η is the ripple height.

Nielsen [1988] also developed a convective transport model [see also *Nielsen*, 1992] for vortex ripple sediment entrainment, which links equation (6) to an exponential probability distribution for the heights reached by particles when they are first entrained by the lee vortex; following their notation, this distribution is denoted $f(z) \propto c(z)$. An additional constraint on $f(z)$ is that the maximum entrainment height should equal the vertical distance of particle settling during one wave stroke, to satisfy the assumption of bed equilibrium. For particles settling at the rate w_s, and neglecting vertical advection by a mean flow, this implies $f(z) = 0$ for $z > \pi w_s/\omega$, where $\omega = 2\pi/T$. Therefore a truncated exponential probability distribution is proposed,

$$f(z) = L_0^{-1}\left(1 - e^{-\pi w'}\right)^{-1} e^{-z/L_0}, \quad 0 < z < \pi w', \tag{8}$$

and $f(z) = 0$ outside of $0 < z < \pi w'$; here, a non-dimensional settling velocity has also been introduced,

$$w' = \frac{w_s}{\omega L_0}. \tag{9}$$

Once entrained, particles are advected with the wave orbital velocity $u = U_0 \sin \omega t$ while settling vertically at speed w_s, so that the total horizontal distance for a particle starting at $z = z_0$ is

$$x(z_0) = A\left(1 - \cos\frac{\omega z_0}{w_s}\right), \tag{10}$$

where $A = U_0/\omega$ is the wave orbital excursion amplitude. Combining equations (8) and (10) yields a distribution for the jump lengths,

$$p_X(x) = \frac{w'}{A}\left(1 - e^{-\pi w'}\right)^{-1} \frac{\exp\left[-w' \cos^{-1}\left(1 - \frac{x}{A}\right)\right]}{\left[1 - \left(1 - \frac{x}{A}\right)^2\right]^{1/2}}, \tag{11}$$

valid for $0 < x < 2A$ (otherwise $p_X(x) = 0$). The mean and variance of jump length can be calculated from p_X as

$$\mu_x = \frac{A}{e^{\pi w'} - 1}\left[\frac{1 + e^{\pi w'}}{1 + w'^2} - 2\right], \tag{12}$$

$$\sigma_x^2 = \frac{2A^2}{e^{\pi w'} - 1}\left[\frac{5 + 3e^{\pi w'} + 2w'^2}{4 + 5w'^2 + w'^4} - 2\right] - \mu_x^2. \tag{13}$$

Figure 8 shows the dependence of mean and variance on w'. This result is used to close equations (3)–(5).

3 Experimental Data: *Miller and Komar* [1979]

The *Miller and Komar* [1979] (hereafter MK79) experiments were among the first to be conducted in the Oregon State University large wave flume, which at that time had width 3.7 m, water depth 3.7 m, and used a paddle wavemaker. The flume was lined with well-sorted beach sand with median grain diameter 0.178 mm, which was brought to an equilibrium bed state consisting of orbital-scale ripples. Fluorescently tagged tracer sand was then added to the equilibrated bed in a narrow transverse line at time $t = 0$. The transverse-averaged spatial distribution of tracer concentration, $C(x, t)$, was measured in synoptic "snapshots" by SCUBA divers collecting grab samples on a regular grid (with the wavemaker

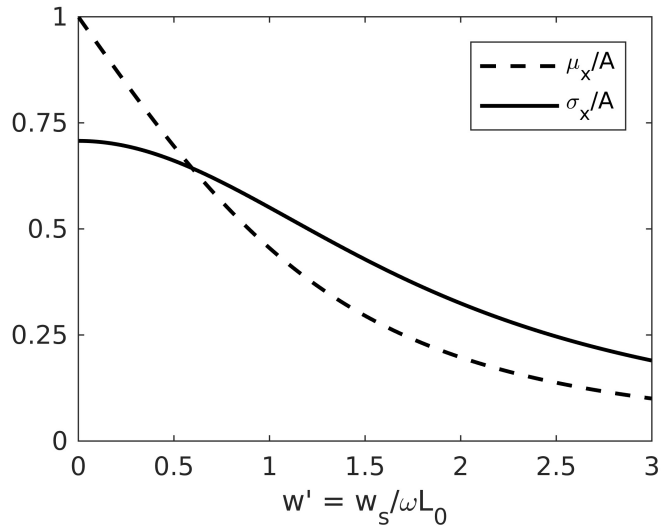

Figure 8. Dependence of moments of particle jump length distribution (equations 12–13) on nondimensional particle settling velocity w', normalized by wave orbital excursion amplitude A.

Table 1. Experimental conditions for MK79 laboratory (Exp. 1–3) and field (Exp. F1–F2) data. Wave parameters for field data are based on significant wave height, used for all calculations.

Exp.	Period T [sec]	Height H [cm]	Orb. Vel. U_0 [cm/s]	Ripple Length λ [cm]	Ripple Amp η [cm]
1	3	37.6	17.5	7.5	1.0
2	4	37.6	24.2	13.5	1.0
3	5	35.1	33.7	10.6	1.0
F1	10	92	26.9	7.3	1.2
F2	10	99	27.0	10.6	1.8

stopped). Four such snapshots were collected spanning 90 minutes of wave action, and this was repeated for three trials with wave periods of 3, 4, and 5 seconds respectively.

Two similar experimental trials were also conducted by MK79 in the field at 16–18 m depth off the Oregon coast. In that case, tracer was placed at a single location and then surveyed once after a period of 60 minutes for each trial. The spreading of tracer in the field was 2-dimensional and nearly isotropic, in contrast to the laboratory data which measured 1-dimensional spreading. Therefore, when comparing to field data the model (section 2) will be modified by adjusting the value of σ_x downwards by a factor of $1/\sqrt{2}$. Effectively this extends the model to 2-dimensions by using the vector sum of two 1-dimensional horizontal random walks, scaled to preserve the magnitude of jump length.

The relevant experimental parameters are listed in Table 1. Note that the ripple height, η, was reported by *Miller and Komar* [1980] for the laboratory data of MK79, but values of η were not recorded for the field experiments. A synthesis of laboratory and field observations of vortex (orbital-scale) ripples by *Wiberg and Harris* [1994] found $\eta \approx 0.17\lambda$ over a broad range of the ripple wavelengths λ, hence this parameterization is used to estimate η for the MK79 field data.

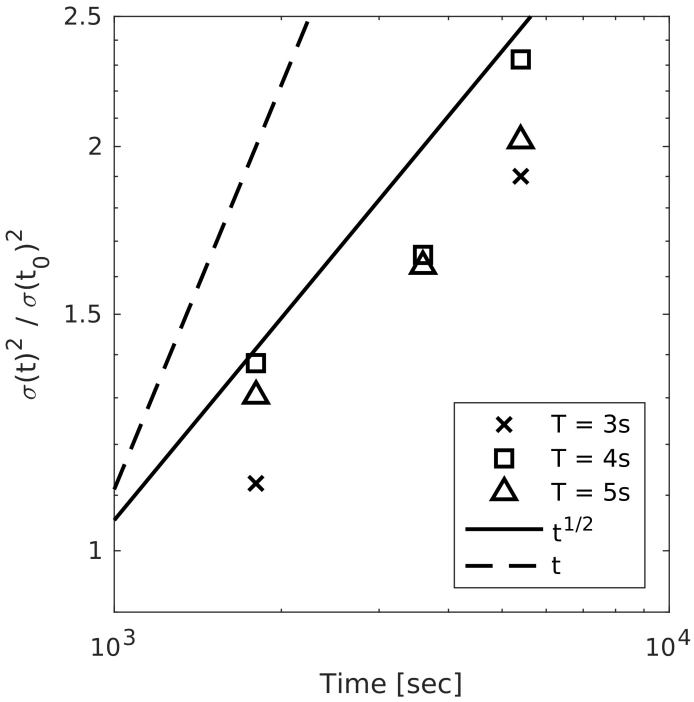

Figure 9. Longitudinal variance of tracer concentration, vs. time, from laboratory measurements of MK79 for three values of wave period T (see legend). Data have been normalized by the variance observed at $t = 900$ s in each case. Solid and dashed lines represent sub-diffusive and classical diffusion models, $t^{1/2}$ and t respectively.

To my knowledge, the MK79 experiments are the only systematic investigation of sand tracer dispersal by waves, controlling for complicating factors such as low-frequency currents or broad grainsize distribution. Other studies using sand tracers in waves have focused on tracer advection as a means to determine net sediment transport, and were not designed in such a way as to isolate the diffusion process. The MK79 experiments were conducted far from the wave breaking zone where undertow might cause a net transport, and the laboratory waves had small Ursell numbers such that the wave velocities were likely highly symmetric. Therefore, the MK79 data alone is used for validating the CTRW model in section 4.

4 Results

Longitudinal tracer variance was estimated by MK79 [tabulated in *Miller*, 1978] based on graphical fits to the raw transverse-averaged observations. These data are compared to the model in two ways. First, Figure 9 shows the variance vs. time for the laboratory experiments, normalized by the variance observed at time $t = 900$ s. This shows that the data collapse to a constant rate of spreading which is roughly $t^{1/2}$, confirming the prediction of the model. Second, Figure 10 compares the dimensional (non-normalized) variance of longitudinal tracer distribution for both laboratory and field data to predictions using equation (5). Note that these results depend on the parameterization used for jump length variance, equation (13), and therefore should be considered a quantitative validation thereof. The relevant model parameters are listed in Table 2, calculated from the experimental parameters listed in Table 1. These calculations assume quartz sand with median grain diameter 0.178 mm as

Table 2. Calculated parameters for MK79 laboratory (Exp. 1–3) and field (Exp. F1–F2) experiments.

Exp.	Time Scale $\Delta t = T/2$	Orb. Amp. A [cm]	Vert. Scale L_0 [cm]	Non-Dim Vel. w' [-]
1	1.5	8.36	0.70	1.3
2	2.0	15.4	0.97	1.2
3	2.5	26.8	1.4	1.1
F1	5	43	1.3	2.2
F2	5	43	2.0	1.5

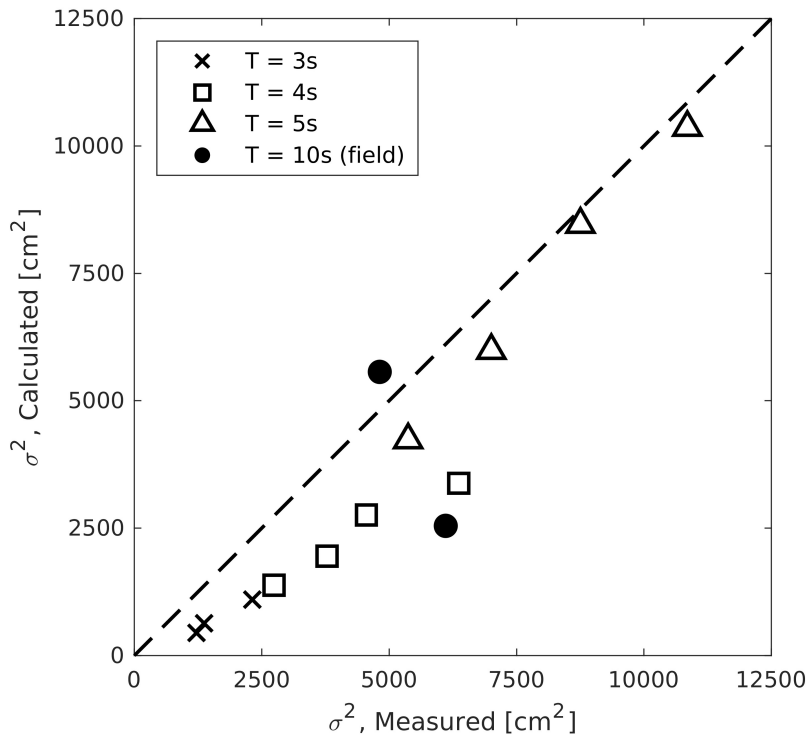

Figure 10. Calculated vs. measured values of longitudinal tracer spread (spatial variance). Calculations use the parameter values listed in Table 2.

reported by MK79, which yielded a settling velocity of 1.87 cm/s using the parameterization by *Brown and Lawler* [2003].

Figure 11 compares the longitudinal distribution of tracer predicted by equation (3) to laboratory observations, for snapshots in time in each MK79 experiment (data were digitized from MK79 Figs. 2–4). Results using classical diffusion theory are also shown, using the constant diffusion coefficients estimated by MK79. Figure 12 shows the same data normalized to unit variance using equation (5). In these figures, the shape of the main lobe of the tracer plume is seen to be generally well-fit by equation (3), and is also well-fit by a Gaussian distribution as predicted by the classical theory. The classical model does not correctly predict the spreading rate of the plume over time, however, as seen in Figures 9 and 11.

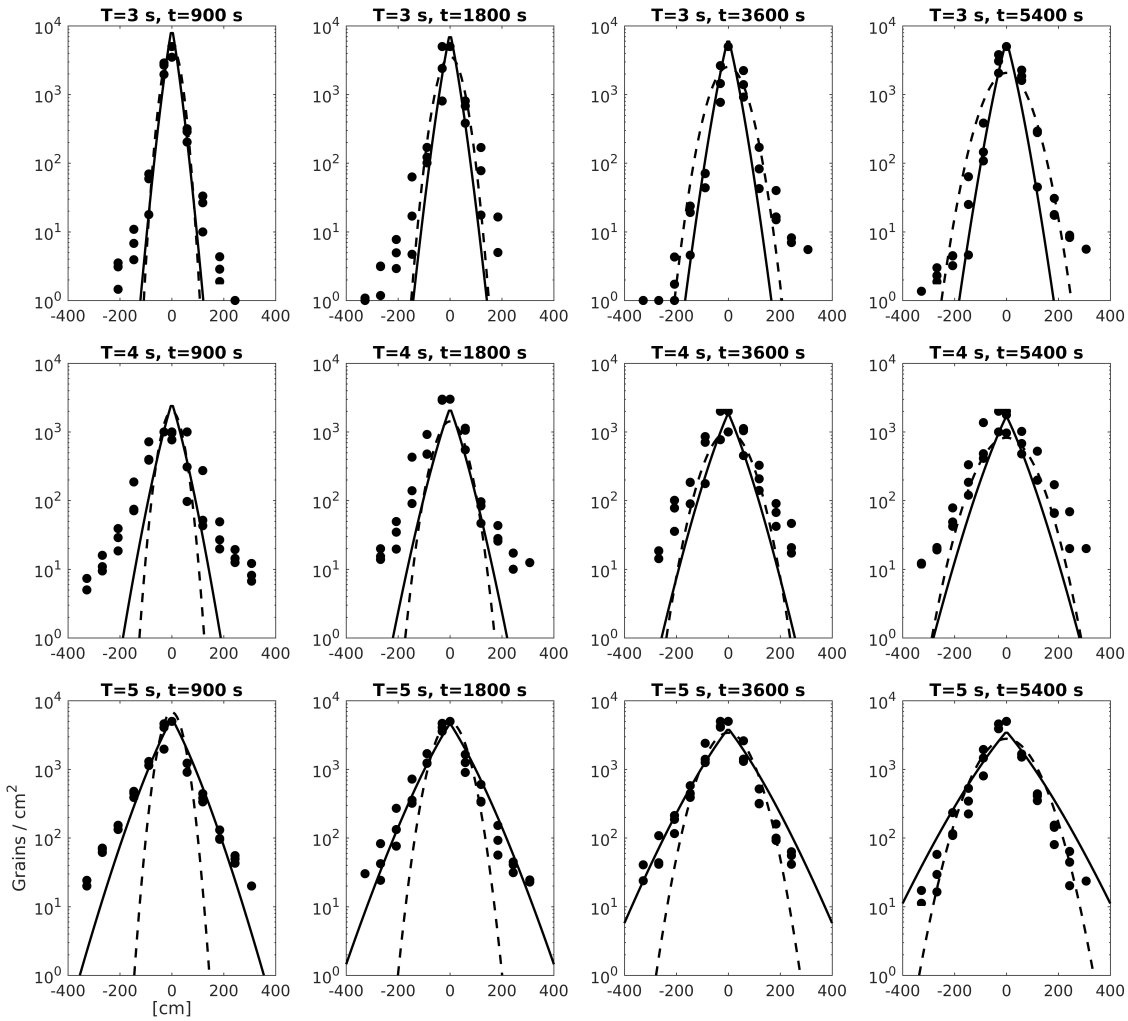

Figure 11. Model-data comparison for snapshots of longitudinal distribution of tracer concentration from MK79 experiments (black dots, representing three longitudinal transects). Solid lines are the distribution predicted by the CTRW model (equation (3)), using parameters listed in Table 2. Dashed lines are Gaussian distributions, using the diffusion coefficient obtained by MK79 by fitting to data for $t \geq 900$. Scaling factor to convert from modeled probability density to measured grains per cm^2 is based on observed total tracer mass at $t = 900$ s, for each experiment. Axis labels in bottom-left apply to all sub-figures.

Both models underpredict the tracer concentration in the tails of the distribution (see Figure 12), in all cases. A possible source for this error lies in the jump length probability distribution in the CTRW model, p_X; in particular, a better overall fit could be obtained by instead assuming a power-law distribution for p_X. To show this, the dashed line in Figure 12 represents a Monte-Carlo integration of the CTRW model with $p_X \sim x^{-1-\beta}$ [sampled following Clauset *et al.*, 2009]. Tests were performed for values of β ranging from 0.5 to 2.5, in increments of 0.1; the results using $\beta = 1.8$ are shown, chosen based on minimizing the mean-square difference in log-probability between theory and observations.

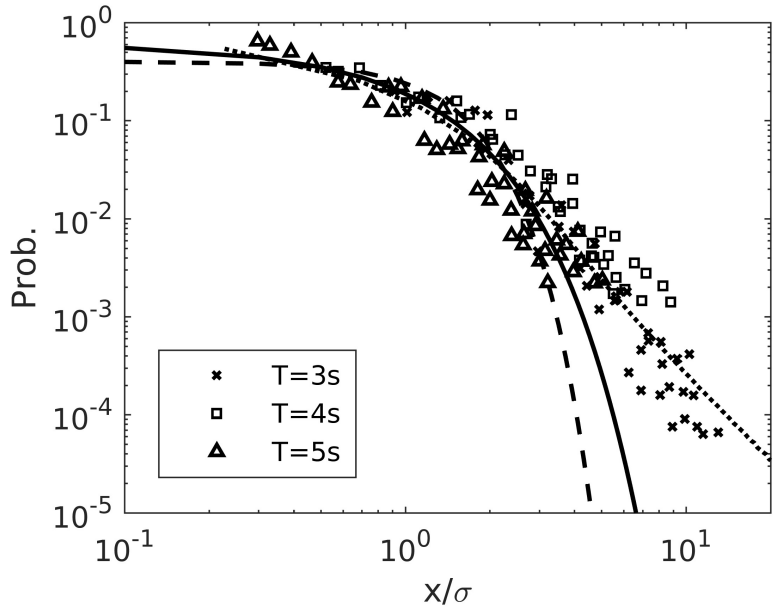

Figure 12. Tracer distribution data as in Figure 11, but normalized to unit variance using equation (5). Solid line is equation (3), dashed line is a Gaussian distribution, and dashed line is computed from a CTRW model with $p_X \sim x^{-1-\beta}$, where $\beta = 1.8$ (see text).

5 Discussion

A major factor distinguishing the present CTRW model from the classical diffusion model is the prediction of sub-diffusion due to particle burial. MK79 observed this qualitatively, and described it in terms of an initially fast rate of tracer spreading followed by a slowdown over time. Figure 9 shows that tracer variance in fact grows roughly as $t^{1/2}$, much slower than the linear growth rate predicted by the classical theory. This has significant implications for long-term particle dispersal. For the field data of MK79, for instance, extrapolating the measured plume by assuming linear variance growth would yield a spread of about 10 meters in 10 days; the same extrapolation using the sub-diffusive model predicts a spread of only about 3 meters. If sub-diffusion does extend to such long time periods, it seems likely it would be quickly overwhelmed by dispersal due to advective transport, which would be an important consideration for Lagrangian models. On the other hand, additional experiments would be needed to confirm that sub-diffusion persists over time. For instance, *Voepel et al.* [2013] showed that a finite maximum depth for particle burial, which is not considered in the present model, leads to a transition to classical diffusion behavior at long time scales, and *Nikora et al.* [2002] also observed regimes of anomalous diffusion behavior that changed depending on time scale.

Figures 9–12 show that the CTRW model reproduces most aspects of the MK79 observations, with some notable exceptions. For field data, errors may have occurred due to the uncertainty of physical parameters, for example the ripple amplitude was not directly measured. The laboratory data are predicted with apparently less error than field data, although the tracer spatial variance was systematically underpredicted compared to measurements (Figure 10), which suggests underprediction of the jump length variance by equation (13). An exception to this systematic trend is the $T = 5$ s experiment, for which the tracer spread was well-predicted. However, it should also be noted that the $T = 5$ s experiment had relatively shorter wavelength ripples, suggesting a possible transition to sub-orbital ripples which would cast doubt on the vortex ripple parameterizations underlying equation (13). Therefore,

it seems likely that jump length variance is generally underpredicted by equation (13), due either to simplifications made by the jump length model (section 2.3), or uncertainty in the parameterizations used to calculate w'. Further investigation of these errors would require measurements of suspended sediment concentration and particle jump length, which were not available for the present experiments.

The model also under-predicted tracer concentrations in the tails of the distribution, Figure 12. This discrepancy, while small in magnitude, is notable because it may point to important physics missing in the proposed model. A working hypothesis is that the assumed particle jump length distribution, p_X, is responsible for this aspect of model-data misfit. In particular a heavy-tailed jump length distribution, i.e. $p_X \propto x^{-1-\beta}$ where $0 < \beta < 2$ (empirically, $\beta = 1.8$), was found to predict the tails of the distribution, despite contrasting with the intuitive notion that jump lengths should be limited by the wave excursion amplitude. Power-law tails have also been observed in tracer distributions in fluvial transport, and hypotheses about p_X have also been put forward in those cases [e.g. see the review by *Schumer et al.*, 2009], although experimental evidence has not yet confirmed such a distribution. Another explanation in that case invokes the combination of heavy-tailed rest time distribution with a thin-tailed but strongly-asymmetric (downstream directed) jump length distribution [*Weeks and Swinney*, 1998; *Phillips et al.*, 2013; *Bradley*, 2017]; this explanation does not require heavy-tailed p_X, but does require asymmetry which was not present in the MK79 experiments. Possibly a different, yet unknown, mechanism exists that can explain the anomalous tail behavior in the oscillatory flow case, for example related to the intermittent bursts of suspension that have been observed to occur in fine sand transport in oscillatory flow [*Jaffe and Sallenger*, 1993; *Cox and Kobayashi*, 2000; *Yoon and Cox*, 2012; *Brinkkemper et al.*, 2016]. It is unclear how such effects would be quantified and modeled, however, and so the more parsimonious heavy-tailed p_X hypothesis is adopted for now. Testing this hypothesis would require more detailed observations of particle trajectories under waves, similar to the unidirectional flow experiments by *Martin et al.* [2012].

6 Conclusions

A random walk model was developed for diffusion of sediment by waves. The main feature of the model is its representation of sediment burial, which tends to slow down diffusion by causing intermittent long rest times between particle motions. By treating the sediment transport as homogeneous and in equilibrium, and being associated with a regular surface time scale (the period of wave motion), the burial duration is found to be equivalent to the first-return time of a 1-dimensional random walk, equation (1). The heavy-tailed nature of this distribution causes the model to predict a sub-diffusive rate of particle spreading, qualitatively different from the predictions of classical diffusion theory as assumed in previous studies.

A simple "grab and dump" style model of sediment transport is used to close the model by providing a probability distribution for the particle jump lengths. This model assumes an initial exponential vertical distribution of particles upon entrainment by a ripple lee vortex, followed by passive horizontal advection and vertical settling. The resulting jump length distribution is cast in terms of a nondimensional settling velocity and the wave orbital excursion amplitude, equations (11)–(13). Both parameters are given in terms of physical properties of the sediment and waves, i.e. no free tuning parameters are included in the model.

The physical validity of the model was tested using a re-analysis of the unique sediment tracer dataset of *Miller and Komar* [1979]. Their measurements confirm the model prediction of sub-diffusive spreading, where the longitudinal variance of tracer concentration grows as $t^{1/2}$. The measured longitudinal variance of the tracer distribution is also well-predicted based on the proposed jump length distribution, and the spatial shape of tracer plumes is for the most part well-fit by either the proposed model or a classical Gaussian distribution. Notably, the tails of the measured tracer plumes were not well-fit by either the

proposed model or the classical Gaussian shape, but could be fit by assuming a heavy-tailed distribution for particle jump length, $p_X \sim x^{-1-\beta}$, where $\beta = 1.8$. This distribution is qualitatively different than what is expected for sediment transport under waves, and this interesting result remains to be explained.

A: Non-Uniform Entrainment Within Ripple Cells

Spatially non-uniform entrainment may be expected to influence the probability distribution of particle rest time, insomuch as particles that are deposited in areas of lower flow or bed slope (e.g., a ripple trough) may take longer to be re-mobilized. This section shows that such effects can be neglected when modeling the long-term statistical behavior of particle trajectories as in section 2.1. The added influence of burial on the particle rest times is not considered in this section, but can be included subsequently following the same logic of section 2.1.

A sediment packet as described in section 2.1 consists of particles mobilized from a variety of positions within a ripple cell, and likewise these particles may be deposited anywhere along the receiving ripple cell. To model this, consider a microscopic lattice discretizing each ripple cell into M sites, denoted by $j = 1, \ldots, M$. During each wave stroke, define a probability mass distribution $p_{m,j}$ which is used to randomly select pM particles for transfer, where p is the transfer probability defined in section 2.1. Upon transfer, $p_{m,j}$ is also used to randomly assign deposition sites in the receiving sub-cell, to satisfy the assumption of equilibrium. Moreover, note that particles are subject to vortex stirring during transfer, so that the site from which a transfer is initiated does not influence the site to which that particle is deposited. Therefore, the site j occupied by a particle at any one time does not influence its later trajectory — for example, a particle entrained from a ripple trough is not preferentially deposited in another ripple trough. Given this, statistics may be calculated on the particle rest times as follows. First consider the probability that a particle at a given site j will rest for N time steps before being selected for transfer:

$$p_{m,j}\left(1 - p_{m,j}\right)^{N-1}. \tag{A.1}$$

After many jumps, a particle will have visited sites j each with probability $p_{m,j}$, hence the average of its rest time between jumps (neglecting burial as noted previously) is proportional to

$$\begin{aligned} E[N] &= \sum_{j=1}^{M} p_{m,j} \sum_{N=1}^{\infty} N p_{m,j}\left(1 - p_{m,j}\right)^{N-1} \\ &= \sum_{j=1}^{M} p_{m,j}^2 \sum_{N=1}^{\infty} N\left(1 - p_{m,j}\right)^{N-1} \\ &= M \end{aligned} \tag{A.2}$$

Similarly, the variance of rest times in the particle's trajectory is proportional to $E[N^2] - E[N]^2$, where

$$\begin{aligned} E\left[N^2\right] &= \sum_{j=1}^{M} p_{m,j} \sum_{N=1}^{\infty} N^2 p_{m,j}\left(1 - p_{m,j}\right)^{N-1} \\ &= \sum_{j=1}^{M} \frac{2 - p_{m,j}}{1 - p_{m,j}} \end{aligned} \tag{A.3}$$

This shows that the rest times have finite variance, so the law of large numbers applies. That is, for a sufficiently large number of wave strokes S the total number of transfer events converges to $N/(pMS)$, i.e. is not dependent on the spatial distribution of entrainment probabilities $p_{m,j}$. The rate of convergence (definition of "large" S) depends, however, on the particular choice of $p_{m,j}$, because large values of rest time variance will result in a longer time for convergence.

Acknowledgments

The author thanks Paul Komar for insightful discussions and background on the experimental data, and Stephen Lancaster for reviewing an early version of the manuscript which greatly improved its presentation. Feedback from David Furbish and two anonymous reviewers greatly improved this article. All of the data used in this article were derived from the cited works by Miller & Komar.

References

Admiraal, D., R. Musalem-Jara, M. García, and Y. Niño (2006), Vortex trajectory hysteresis above self-formed vortex ripples, *Journal of Hydraulic Research*, *44*(4), 437–450.

Allan, J. C., R. Hart, and J. V. Tranquili (2006), The use of passive integrated transponder (pit) tags to trace cobble transport in a mixed sand-and-gravel beach on the high-energy oregon coast, usa, *Marine Geology*, *232*(1), 63–86.

Ancey, C. (2010), Stochastic modeling in sediment dynamics: Exner equation for planar bed incipient bed load transport conditions, *Journal of Geophysical Research: Earth Surface*, *115*(F2).

Ancey, C., T. Böhm, M. Jodeau, and P. Frey (2006), Statistical description of sediment transport experiments, *Physical Review E*, *74*(1), 011,302.

Ancey, C., A. Davison, T. Böhm, M. Jodeau, and P. Frey (2008), Entrainment and motion of coarse particles in a shallow water stream down a steep slope, *Journal of Fluid Mechanics*, *595*, 83–114.

Bagnold, R. A., and G. Taylor (1946), Motion of waves in shallow water. interaction between waves and sand bottoms, *Proceedings of the Royal Society of London. Series A, Mathematical and Physical Sciences*, pp. 1–18.

Ballio, F., and A. Radice (2015), Fluctuations and time scales for bed-load sediment motion over a smooth bed, *International Journal of Sediment Research*, *30*(4), 321–327.

Bradley, D. N., G. E. Tucker, and D. A. Benson (2010), Fractional dispersion in a sand bed river, *Journal of Geophysical Research: Earth Surface*, *115*(F1).

Bradley, D. N. (2017), Direct observation of heavy-tailed storage times of bed load tracer particles causing anomalous superdiffusion, *Geophysical Research Letters*, *44*(24).

Brinkkemper, J., A. de Bakker, and B. Ruessink (2016), Intra-wave sand suspension in the shoaling and surf zone of a field-scale laboratory beach, *Journal of Geophysical Research: Earth Surface*.

Brown, P. P., and D. F. Lawler (2003), Sphere drag and settling velocity revisited, *Journal of Environmental Engineering*, *129*(3), 222–231.

Clauset, A., Shalizi, C.R. & Newman, M.E. (2009). Power-law distributions in empirical data. *SIAM review*, **51**, 661–703.

Cox, D. T., and N. Kobayashi (2000), Identification of intense, intermittent coherent motions under shoaling and breaking waves, *Journal of Geophysical Research: Oceans*, *105*(C6), 14,223–14,236.

Drake, T. G., R. L. Shreve, W. E. Dietrich, P. J. Whiting, and L. B. Leopold (1988), Bedload transport of fine gravel observed by motion-picture photography, *Journal of Fluid Mechanics*, *192*, 193–217.

Earnshaw, H., and C. Greated (1998), Dynamics of ripple bed vortices, *Experiments in Fluids*, *25*(3), 265–275.

Einstein, H. (1937), Bedload transport as a probability problem, *Sedimentation (reprinted in 1972). Water Resources Publications, Colorado*, pp. 105–108.

Fan, N., D. Zhong, B. Wu, E. Foufoula-Georgiou, and M. Guala (2014), A mechanistic-stochastic formulation of bed load particle motions: From individual particle forces to the Fokker-Planck equation under low transport rates, *Journal of Geophysical Research: Earth Surface*, *119*(3), 464–482.

Fan, N., A. Singh, M. Guala, E. Foufoula-Georgiou, and B. Wu (2016), Exploring a semimechanistic episodic langevin model for bed load transport: Emergence of normal

and anomalous advection and diffusion regimes, *Water Resources Research*, *52*(4), 2789–2801.

Fathel, S. L., D. J. Furbish, and M. W. Schmeeckle (2015), Experimental evidence of statistical ensemble behavior in bed load sediment transport, *Journal of Geophysical Research: Earth Surface*, *120*(11), 2298–2317.

Furbish, D. J., and M. W. Schmeeckle (2013), A probabilistic derivation of the exponential-like distribution of bed load particle velocities, *Water Resources Research*, *49*(3), 1537–1551.

Gallagher, E. L. (2011), Computer simulations of self-organized megaripples in the nearshore, *Journal of Geophysical Research: Earth Surface*, *116*(F1).

Ganti, V., M. M. Meerschaert, E. Foufoula-Georgiou, E. Viparelli, and G. Parker (2010), Normal and anomalous diffusion of gravel tracer particles in rivers, *Journal of Geophysical Research: Earth Surface*, *115*(F2).

Habersack, H. (2001), Radio-tracking gravel particles in a large braided river in new zealand: A field test of the stochastic theory of bed load transport proposed by einstein, *Hydrological Processes*, *15*(3), 377–391.

Hassan, M. A., H. Voepel, R. Schumer, G. Parker, and L. Fraccarollo (2013), Displacement characteristics of coarse fluvial bed sediment, *Journal of Geophysical Research: Earth Surface*, *118*(1), 155–165.

Heyman, J., F. Mettra, H. Ma, and C. Ancey (2013), Statistics of bedload transport over steep slopes: Separation of time scales and collective motion, *Geophysical Research Letters*, *40*(1), 128–133.

Hill, K., L. DellAngelo, and M. M. Meerschaert (2010), Heavy-tailed travel distance in gravel bed transport: An exploratory enquiry, *Journal of Geophysical Research: Earth Surface*, *115*(F2).

Ingle, J., and D. Gorsline (1973), Use of fluorescent tracers in the near-shore environment, *Tracer Techniques in Sediment Transport*, pp. 125–148.

Inman, D., and T. Chamberlain (1959), Tracing beach sand movement with irradiated quartz, *Journal of Geophysical Research*, *64*(1), 41–47.

Jaffe, B., and A. Sallenger (1993), The contribution of suspension events to sediment transport in the surf zone, in *Proc. 23rd Int. Coastal Eng. Conf.*, pp. 2680–2693, Am. Soc. Civil Eng., Venice.

Klafter, J., and I. M. Sokolov (2011), *First steps in random walks: From tools to applications*, Oxford University Press.

Komar, P. D. (1969), The longshore transport of sand on beaches, Ph.D. thesis, University of California, San Diego.

Komar, P. D., and D. L. Inman (1970), Longshore sand transport on beaches, *Journal of Geophysical Research*, *75*(30), 5914–5927.

Lajeunesse, E., L. Malverti, and F. Charru (2010), Bed load transport in turbulent flow at the grain scale: Experiments and modeling, *Journal of Geophysical Research: Earth Surface*, *115*(F4).

Martin, R. L., D. J. Jerolmack, and R. Schumer (2012), The physical basis for anomalous diffusion in bed load transport, *Journal of Geophysical Research: Earth Surface*, *117*(F1).

Martin, R. L., P. K. Purohit, and D. J. Jerolmack (2014), Sedimentary bed evolution as a mean-reverting random walk: Implications for tracer statistics, *Geophysical Research Letters*, *41*(17), 6152–6159.

Mazumder, B., and S. Paul (2012), Dispersion of settling particles in oscillatory turbulent flow subject to deposition and re-entrainment, *European Journal of Mechanics-B/Fluids*, *31*, 80–90.

McComb, P., and K. Black (2005), Detailed observations of littoral transport using artificial sediment tracer, in a high-energy, rocky reef and iron sand environment, *Journal of Coastal Research*, pp. 358–373.

Mei, C. C., and C. Chian (1994), Dispersion of small suspended particles in a wave boundary layer, *Journal of Physical Oceanography*, *24*(12), 2479–2495.

Metzler, R., and J. Klafter (2000), The random walk's guide to anomalous diffusion: a fractional dynamics approach, *Physics reports*, *339*(1), 1–77.

Miller, M. C. (1978), Laboratory and field investigations on the movement of sand tracer under the influence of water waves: ripple development and longitudinal spreading of tracer material, Ph.D. thesis.

Miller, M. C., and P. D. Komar (1979), Measurements of sand spreading rates under near-bottom wave orbital motions, *Journal of Geology*, *87*(6), 593–608.

Miller, M. C., and P. D. Komar (1980), Oscillation sand ripples generated by laboratory apparatus, *Journal of Sedimentary Research*, *50*(1).

Montroll, E. W., and G. H. Weiss (1965), Random walks on lattices. ii, *Journal of Mathematical Physics*, *6*(2), 167–181.

Nakato, T., J. F. Kennedy, J. R. Glover, and F. A. Locher (1977), Wave entrainment of sediment from rippled beds, *Journal of the Waterway, Port, Coastal and Ocean Division*, *103*(1), 83–99.

Nielsen, P. (1988), Three simple models of wave sediment transport, *Coastal Engineering*, *12*(1), 43–62.

Nielsen, P. (1992), *Coastal bottom boundary layers and sediment transport*, vol. 4, World Scientific Publishing Company.

Nikora, V., H. Habersack, T. Huber, and I. McEwan (2002), On bed particle diffusion in gravel bed flows under weak bed load transport, *Water Resources Research*, *38*(6).

Osborne, P. D. (2005), Transport of gravel and cobble on a mixed-sediment inner bank shoreline of a large inlet, Grays Harbor, Washington, *Marine Geology*, *224*(1), 145–156.

Pannell, M., T. O'Hare, and D. Huntley (2002), Modelling sand ripple development by self-organization in unsteady flows, in *Proceedings Coastal Engineering*, pp. 2837–2849.

Parker, G., C. Paola, and S. Leclair (2000), Probabilistic exner sediment continuity equation for mixtures with no active layer, *Journal of Hydraulic Engineering*, *126*(11), 818–826.

Pelosi, A., G. Parker, R. Schumer, and H.-B. Ma (2014), Exner-based master equation for transport and dispersion of river pebble tracers: Derivation, asymptotic forms, and quantification of nonlocal vertical dispersion, *Journal of Geophysical Research: Earth Surface*, *119*(9), 1818–1832.

Pelosi, A., R. Schumer, G. Parker, and R. Ferguson (2016), The cause of advective slowdown of tracer pebbles in rivers: Implementation of exner based master equation for coevolving streamwise and vertical dispersion, *Journal of Geophysical Research: Earth Surface*.

Phillips, C. B., R. L. Martin, and D. J. Jerolmack (2013), Impulse framework for unsteady flows reveals superdiffusive bed load transport, *Geophysical Research Letters*, *40*(7), 1328–1333.

Pizzuto, J. E. (1987), Dispersion of dyed sand tracers in an oscillatory flow field, *Journal of Geophysical Research: Oceans*, *92*(C2), 1923–1933.

Radice, A., V. Nikora, J. Campagnol, and F. Ballio (2013), Active interactions between turbulence and bed load: Conceptual picture and experimental evidence, *Water Resources Research*, *49*(1), 90–99.

Roseberry, J. C., M. W. Schmeeckle, and D. J. Furbish (2012), A probabilistic description of the bed load sediment flux: 2. Particle activity and motions, *Journal of Geophysical Research: Earth Surface*, *117*(F3).

Schumer, R., M. M. Meerschaert, and B. Baeumer (2009), Fractional advection-dispersion equations for modeling transport at the earth surface, *Journal of Geophysical Research: Earth Surface*, *114*(F4).

Soulsby, R., C. Mead, and B. Wild (2007), A model for simulating the dispersal tracks of sand grains in coastal areas: âĂŸSandTrackâĂŹ, *Geological Society, London, Special Publications*, *274*(1), 65–72.

Stark, N., and A. E. Hay (2016), Pebble and cobble transport on a steep, mega-tidal, mixed sand and gravel beach, *Marine Geology*, *382*, 210–223.

Thorne, P. D., A. G. Davies, and P. S. Bell (2009), Observations and analysis of sediment diffusivity profiles over sandy rippled beds under waves, *Journal of Geophysical Research:*

Oceans, *114*(C2).

Tucker, G. E., and D. N. Bradley (2010), Trouble with diffusion: Reassessing hillslope erosion laws with a particle-based model, *Journal of Geophysical Research: Earth Surface*, *115*(F1).

van der Werf, J. J., J. S. Ribberink, T. O'Donoghue, and J. S. Doucette (2006), Modelling and measurement of sand transport processes over full-scale ripples in oscillatory flow, *Coastal engineering*, *53*(8), 657–673.

van der Werf, J. J., J. Doucette, T. O'Donoghue, and J. S. Ribberink (2007), Detailed measurements of velocities and suspended sand concentrations over full-scale ripples in regular oscillatory flow, *Journal of Geophysical Research: Earth Surface*, *112*(F2).

Voepel, H., R. Schumer, and M. A. Hassan (2013), Sediment residence time distributions: Theory and application from bed elevation measurements, *Journal of Geophysical Research: Earth Surface*, *118*(4), 2557–2567.

Weeks, E. R., and H. L. Swinney (1998), Anomalous diffusion resulting from strongly asymmetric random walks, *Physical Review E*, *57*(5), 4915.

White, T. E. (1998), Status of measurement techniques for coastal sediment transport, *Coastal Engineering*, *35*(1), 17–45.

Wiberg, P. L., and C. K. Harris (1994), Ripple geometry in wave-dominated environments, *Journal of Geophysical Research: Oceans*, *99*(C1), 775–789.

Wilson, G., and A. Hay (2016), Acoustic observations of near-bed sediment concentration and flux statistics above migrating sand dunes, *Geophysical Research Letters*, *43*(12), 6304–6312.

Yoon, H.-D., and D. T. Cox (2012), Cross-shore variation of intermittent sediment suspension and turbulence induced by depth-limited wave breaking, *Continental Shelf Research*, *47*, 93–106.